Citation: Clin Transl Sci (2021) 14, 2075–2084; doi:10.1111/cts.12765

ARTICLE

Hydrazinocurcumin Induces Apoptosis of Hepatocellular Carcinoma Cells Through the p38 MAPK Pathway

Hongtao He[1,†], Kuangyuan Qiao[2,†], Chao Wang[1], Wuhan Yang[1], Zhuo Xu[1], Zhilei Zhang[1], Yuming Jia[1], Chong Zhang[1] and Li Peng[1,*]

Hydrazinocurcumin (HZC), a synthetic derivative of curcumin (CUR), has been documented to show anticancer potential in impeding tumor growth in several cancers, including hepatocellular carcinoma (HCC). However, the underlying molecular mechanisms remain unclear. This study aimed to explore the function and underlying mechanisms of HZC on HCC cells, which may involve the p38 mitogen activated protein kinase (MAPK) pathway. HZC was first purified and identified. HepG2 cells were then subjected to treatment with HZC or CUR of different concentrations and p38 MAPK signaling inhibitor (SB203580) to verify their effects on HCC cell apoptosis and proliferation. Furthermore, the functional relevance between HZC and the p38 MAPK pathway in HCC was examined. It was observed that 40 μM HZC exhibited the best pro-apoptosis effect in HCC cells. HZC was found to inhibit HCC cell proliferation and promote apoptosis, the effect of which was stronger than 5-fluorouracil (5-FU). More importantly, the anti-oncogenic effect of HZC and 5-FU was implicated with activation of the p38 MAPK pathway. *In vivo* experimental results showed that HZC inhibited tumor growth more effectively than 5-FU through the p38 MAPK pathway. These results provide evidence that HZC exerted anti-oncogenic and pro-apoptosis effects in HCC cells through activation of the p38 MAPK pathway.

Study Highlights

WHAT IS THE CURRENT KNOWLEDGE ON THE TOPIC?
☑ Hepatocellular carcinoma (HCC) is a frequently occurring malignancy with a significant impact on public health worldwide. New evidence suggests that inhibition of the p38 mitogen activated protein kinase (MAPK) pathway may have a protective effect on HCC. Hydrazinocurcumin (HZC) is a patented multi-active compound isolated from plants.

WHAT QUESTION DID THIS STUDY ADDRESS?
☑ The purpose of our study is to explore the effects and the underlying mechanisms of HZC on HCC cells through the p38 MAPK pathway.

WHAT DOES THIS STUDY ADD TO OUR KNOWLEDGE?
☑ These results provided evidence that HZC could lead to activation of the p38 MAPK pathway, thus inducing cell apoptosis and alleviating HCC.

HOW MIGHT THIS CHANGE CLINICAL PHARMACOLOGY OR TRANSLATIONAL SCIENCE?
☑ This study provides a new drug target for the treatment of HCC with natural products.

Hepatocellular carcinoma (HCC) is the third leading cause of cancer-related deaths around the world, with an estimated incidence of 749,000 new cases each year.[1] At present, the prognosis of HCC remains unfavorable with an average survival rate of 6–12 months.[2] The risk factors responsible for occurrence of HCC have shown association with viral hepatitis infection, excessive alcohol intake, and nonalcoholic cirrhosis, all of which also increase the morbidity of HCC.[3] Currently, clinical approaches combating HCC include systemic or local chemotherapy, radiotherapy, radiofrequency ablative surgery, partial hepatectomy, and liver transplantation.[4] Unfortunately, despite advances in therapy options for the treatment of HCC, the current chemotherapy methods choice for HCC remains less than satisfactory.[5]

Accumulating evidences have identified natural products from medicinal plants like sasanquasaponin,[6] guggulsterone,[7] xanthohumol,[8] and isoliensinine polyphyllin VII[9] as treatment options for tumors for their antiproliferative activities in different human tumor cell lines. Curcumin (CUR) is a yellow chemical isolated from the spice *Curcuma longa.* In addition, CUR has been widely used in pharmaceutical and medical applications due to its nontoxicity and extensive spectrum of biological functions, including antifungal, antibacterial, antiviral, anti-amyloid, antioxidant, and antitumor, as well as anti-inflammatory activities.[10,11] Moreover, modern advances have isolated hydrazinocurcumin (HZC), a patented multi-active compound and an effective derivative of CUR, which might possibly exert antitumor roles

†These authors contributed equally to this work.

[1]Department of Hepatobiliary Surgery, Fourth Hospital of Hebei Medical University Tumor Hospital of Hebei Province, Shijiazhuang, China; [2]Basic Medical College of Hebei Medical University, Shijiazhuang, China. *Correspondence: Li Peng (pengli72@sina.com)
Received: July 23, 2019; accepted: December 16, 2019. doi:10.1111/cts.12765

as well.[12] HZC has been found to reduce an array of downstream targets of STAT3 that suppress cell proliferation and induce cell apoptosis in breast cancer *in vitro.*[13] Moreover, CUR has been highlighted to prevent regional myocardial ischemia/reperfusion injury through inhibition of the p38 mitogen activated protein kinase (MAPK) pathway.[14] The p38 MAPK is a serine threonine kinase that functions as an important mediator of proliferation and apoptosis in several different types of cancer cells.[15] Activation of the p38 MAPK pathway has also been documented to induce apoptotic changes in cisplatin-resistant ovarian cancer cells.[16] Therefore, the current study aimed to investigate the impact of HZC and the p38 MAPK pathway on the progression of HCC and to elucidate a deeper understanding of the biological characteristics of HZC's involvement in the progression of HCC.

METHODS

Preparation, purification, and identification of HZC

With CUR as substrate, the compound was mixed with ethanol and hydrazine hydrochloride and incubated for 7 hours. After being washed with distilled water, the purified compound was filtered and concentrated in vacuum, and extracted with ethyl acetate and multistep column chromatography. The purified compound was further purified using liquid chromatography. Subsequently, the structure of the compound was visualized by infrared spectroscopy, with molecular quality and purity determined by mass spectrometry and liquid chromatography, respectively.

Toxicological experiment

Male Sprague-Dawley (SD) rats (aged 8 weeks, weighing 200–250 g) purchased from Shanghai Institute of Pharmaceutical Industry (Shanghai, China) were allowed to acclimatize to specific pathogen-free conditions with free access to sterilized food and water on laminar flow cabinets. All animal experimentation protocols were approved by the animal ethics committee of the Fourth Hospital of Hebei Medical University. Subsequently, the SD rats were randomly divided into the control and HZC groups (5 rats each). Rats in the HZC group were intraperitoneally administered HZC (80 mg/kg),[17] whereas the rats in the control group were injected with normal saline for a duration of 4 weeks, three times each week. The rats were euthanized after 2 weeks, and the functions of livers and kidneys were tested by measuring the levels of alanine aminotransferase (ALT), aspartate aminotransferase (AST), creatinine (CRE), albumin (ALB), blood urea nitrogen (BUN), and total bilirubin (TBL) using an automatic biochemical analyzer according to kits purchased from Beijing Leadman Biochemical (Beijing, China).

Hematoxylin-eosin staining

Heart, liver, lung, and kidney specimens were fixed with 4% paraformaldehyde and sliced into 5-μm-thick serial sections. Next, myocardial tissues, hepatocyte, superior lobe of right lung tissues, and kidney parenchymal tissues were subjected to hematoxylin-eosin staining. The stained sections were finally observed under a light microscope.

Cell culture and grouping

HepG2 cells from the Shanghai Cell Bank of Chinese Academy of Sciences (Shanghai, China) were cultured in a humified incubator at 37°C with 5% CO_2 in air and Roswell Park Memorial Institute 1640 medium containing 10% fetal bovine serum, 100 μg/mL penicillin, and 100 μg/mL streptomycin. The cells were passaged every 2–3 days and those at the logarithmic phase of growth were selected for subsequent experimentation. Next, the cells were incubated with 20 μM CUR (Sigma-Aldrich Chemical, St. Louis, MO) or 10–40 μM HZC or 1 μg/mL 5-fluorouracil (5-FUl; Shanghai Aladdin Bio-Chem Technology, Shanghai, China) for 24 hours.

To study whether HZC had a concentration-dependent effect on apoptosis of HepG2 cells, cells were respectively incubated with 20 μM CUR, or 10, 20, 40, 50, and 60 μM HZC for 24 hours. Aiming to identify whether HZC affected apoptosis of HepG2 cells through the p38 MAPK pathway, the cells were incubated with dimethylsulfoxide for 24 hours (control group), or with 40 μM HZC for 24 hours (HZC group), or with 5 μmol/L p38 MAPK signaling inhibitor SB203580 (SB203580 group), or with 5 μmol/L SB203580 and 40 μM HZC (HZC + SB203580 group), or with 1 μg/mL 5-FU for 24 hours (5-FU group).

Flow cytometric analysis for cell apoptosis and cell cycle

Annexin V-fluorescein isothiocyanate/propidium iodide (PI) double staining kits were used to detect the apoptosis of the treated cells. First, the cultured cells were suspended and incubated with 5 μL Annexin V-fluorescein isothiocyanate at room temperature avoiding exposure to light. Next, 5 μL PI was added to the cells 5 minutes prior to detection on a Flow Cube 6 cytometer (Sysmex Partec, Germany). In terms of cell cycle detection, the suspended cells were treated with 100 μL RNase A for 30 minutes at 37°C and incubated with 400 μL PI staining solution in darkness at 4°C for 30 minutes. Subsequently, the cell cycle distribution was detected using a flow cytometer.

TUNEL assay

TUNEL assay was applied using *in situ* cell death detection kits (11684795910; Roche, Basel, Switzerland). The cultured cells were treated with 0.1% Triton X-100 (Beyotime Institute of Biotechnology, Shanghai, China) at 4°C for 3 minutes, and then incubated with the TUNEL solution avoiding exposure to light at 37°C for 1 hour. The cells were sealed with antifluorescence quenching sealing solution and then observed under a fluorescence microscope. At last, five visual fields were randomly selected and photographed. The Image J software was adopted to count the number of TUNEL-positive cells in the photographed fields.

EdU assay

Cell proliferation was measured in accordance with the instructions of the EdU Apollo DNA *in vitro* kits. Each well was added with the EdU medium and incubated for 2 hours, and further incubated with glycine for 10 minutes. Next, the cells were incubated with 1 × Apollo staining reaction solution in subdued light for 30 minutes, and then treated with

1 × Hoechst reaction solution avoiding exposure to light for 10 minutes. Cell proliferation was observed under a fluorescence microscope or flow cytometer, and analyzed using the Image Pro Plus 6 software.

Transmission electron microscope for ultrastructure observation

HepG2 cells were incubated with dimethylsulfoxide for 24 hours, and fixed with 2.5% glutaraldehyde for 12 hours, and later with 1% osmium tetroxide at 4°C for 2 hours. After rapid staining with uranium acetate, the cells were dehydrated, and the liquid was renewed thrice. The cells were embedded and sliced before double staining with uranium acetate and lead citrate, followed by observation of the ultrastructural changes under an H-600IV transmission electron microscope (Hitachi, Tokyo, Japan).

RNA isolation and quantitation

Total RNA content of HepG2 cells was extracted using the Trizol method. Based on the instructions of the PrimeScript RT reagent kit with gDNA Eraser kit (Takara Holdings, Kyoto, Japan), the extracted RNA was reserve transcribed into cDNA. Reverse transcription quantitative polymerase chain reaction (RT-qPCR) was performed with the SYBR Premix Ex Taq (Tli RNaseH Plus) kit (Takara Holdings). The fold changes were calculated using relative quantification ($2^{-\triangle\triangle Ct}$ method) with β-actin serving as the internal reference. The primers (**Table S1**) were provided by Shanghai GenePharma (Shanghai, China).

Western blot analysis

Total extracted protein content from the cells and tissues was separated with polyacrylamide gel electrophoresis and electroblotted onto PVDF membrane (Amersham plc, Buckinghamshire, UK), which was then blocked with 5% skimmed milk for 1 hour. The membrane was then probed with the following primary rabbit antibodies: p-p38 (1: 1000, ab178867), p-extracellular signal-regulated kinase (ERK; 1: 1000, ab201015), c-Jun N-terminal kinase (JNK; 1: 1000, ab179461), and p-JNK (1: 1000, ab124956), cleaved caspase 3 (1: 500, ab2302), pro-caspase-3 (1: 1000, ab32499), and mouse antibody against p38 (1: 1000, ab31828), ERK (1: 1000, ab54230), p53 (1: 1000, ab1101), and β-actin (1: 1000, ab8226; **Table S2**). All the above-mentioned antibodies were purchased from Abcam (Cambridge, UK). Then, the membrane was subjected to incubation with horseradish peroxidase-labeled secondary goat anti-mouse or goat anti-rabbit antibody (ab6721/ab205719; Abcam) at ambient temperature for 1 hour. Subsequently, the blots were developed with an optical luminescence analyzer (GE Global Research, Niskayuna, NY), and quantified using the Image Pro Plus 6.0 software.

Xenograft tumor formation in nude mice

The BALB/c-nu/nu nude mice (aged 4 weeks; purchased from Beijing Huafukang Biotechnology (Beijing, China; Animal license No.: CXK 2009-0007) were fed sterilized food and water on a specific pathogen-free laminar flow rack and housed under conditions with constant temperature (24–26°C) and constant humidity (45–55%).

A total of 30 nude mice were divided into 6 groups and subcutaneously inoculated according to their respective grouping. Briefly, the nude mice were intraperitoneally anesthetized with 2% sodium pentobarbital (Beijing Propbs Biotechnology, Beijing, China) at 40 mg/kg. The cells were suspended with concentration adjusted to 2×10^{10} cells/L. Then, 0.2 mL of cells (4×10^6 cells) were subcutaneously injected into the left scapula of each mouse using a 1 mL empty needle for transplantation tumor model establishment. The mice were then randomly divided into the following six groups: negative control (treatment of 80 mg/kg normal saline, 3 times/week), high-dose HZC (treatment of 80 mg/kg, 3 times/week), 5-FU positive control (treatment of 25 mg/kg 5-FU), SB203580 (treatment of 5 μmol/L SB203580, an inhibitor of the p38 MAPK pathway), and HZC + SB203580 (co-treatment of 5 μmol/L SB203580 and 80 mg/kg HZC). Treatment time lasted 4 weeks and the administration was conducted by intraperitoneal injection. From the beginning of injection, the tumor size was measured every 3 days, and a tumor growth curve was drawn. When the tumor volume reached ~ 1,000 mm^3, the nude mice were euthanized, and blood samples were obtained from the heart before death.[18] Levels of ALT, AST, CRE, ALB, BUN, and TBL were measured in order to evaluate pharmacokinetics, efficacy, and toxicity parameters of HZC. The maximum length and vertical short diameter (mm) of tumor were denoted by *a* and *b*, respectively, and measured with a Vernier caliper. The tumor volume (*V*) was calculated according to the following formula: $V = a \times b^2 \times 0.5$.

Immunohistochemistry

Paraffin sections of HCC tissues were dewaxed and hydrated, and treated with diluted potassium citrate solution for antigen repair at 90°C for 10 minutes. Next, the sections were incubated with 3% H_2O_2 for 10 minutes to terminate endogenous peroxidase activity, blocked with 5% goat serum (Beijing Solarbio Science & Technology, Beijing, China) for 20 minutes, and incubated with mouse anti-proliferating cell nuclear antigen (PCNA; 1: 10,000, ab29; Abcam) overnight at 4°C. After incubation with goat anti-mouse working solution (ZSGB-Bio, Beijing, China), the sections were developed with diaminobenzidine and analyzed with a multifunctional true color cell image analysis system (Media Cybernetics, Rockville, MD).

Statistical analysis

All data were processed using the SPSS 21.0 statistical software (IBM, Armonk, NY). Measurement data were expressed as mean ± SD and considered to be statistically significant at $P < 0.05$. Comparisons between the two groups were analyzed using the independent sample *t*-test, whereas comparisons among multiple groups were assessed by one-way analysis of variance.

RESULTS

Purification and characterization of HZC

The structure of HZC is shown in **Figure 1a**. The infrared spectrum demonstrated the disappearance of 1,820–1,600 cm^{-1} C = O peak, indicating that CUR was successfully converted to HZC. The N-H stretching vibration

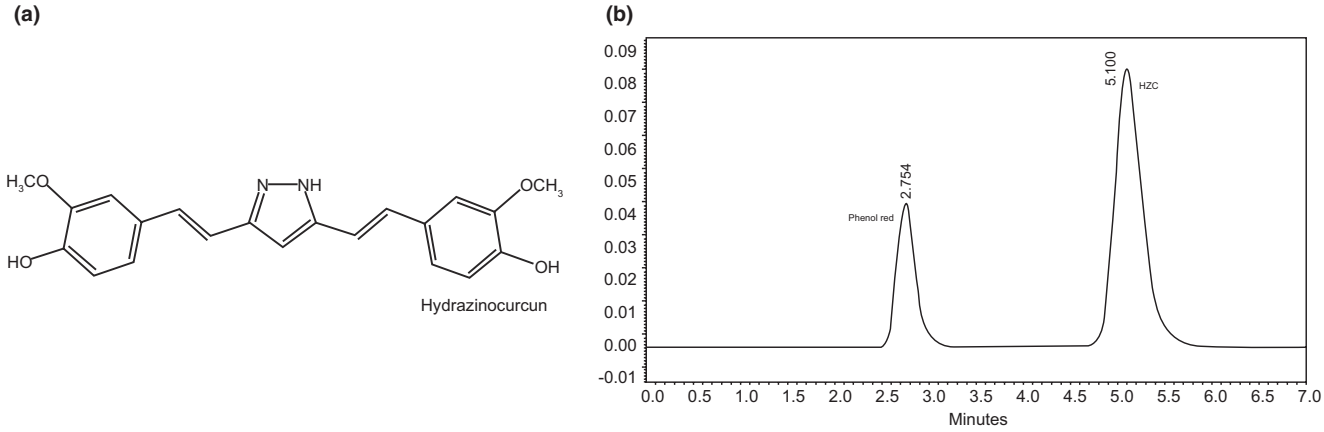

Figure 1 Successful purification of hydrazinocurcumin (HZC). (**a**) Chemical structure of HZC; (**b**) separation and purification of HZC by high-performance liquid chromatography.

peak of 3,319 cm^{-1} was sharp, possibly due to the presence of O-H. In addition, O-H peak at 3,479 cm^{-1}, and 1,593 cm^{-1} presented with N-H bending vibration peak. The ^1H NMR spectrum showed 7.16 (2H, CH_{phenol}), 6.76 (2H, d), 6.97 (2H, dd), 7.09 (2H, d), 6.95 (2H, d), 6.64 (1H, s), and 3.86 (6H, s, OMe). Mass spectrometry results revealed that the molecular mass of the compound was 365. The purity of the compound was further evaluated using liquid chromatography, which (**Figure 1b**) displayed that the obtained compound had a purity of ≥ 97%.

HZC has little toxicity *in vivo*

Determining the levels of ALT, AST, CRE, ALB, BUN, and TBL revealed no significant differences (**Table S3**). The histological images of different tissues in both groups are shown in **Figure 2**. There were no obvious pathological changes, such as injury, inflammation, and necrosis in the HZC group relative to the normal group. As a result, it was deemed that 80 mg/kg dosage of HZC would cause no significant organ damage in mice within 2 weeks, with little toxicity *in vivo*.

The effects of CUR and HZC on apoptosis of HepG2 cells

Cell apoptosis was measured using TUNEL staining and the Annexin-V/PI double staining method. TUNEL results demonstrated that the nuclei of cells were clear and round or oval in shape, and the chromatin was uniformly distributed in the control group. However, in the CUR and HZC groups, some of the nuclei were condensed with crescent or spherical shapes, and the chromatin was aggregated to form granular clusters (**Figure 3a,c**). Subsequently, HepG2 cells were treated with different concentrations of HZC, which suggested that apoptosis was the strongest at the concentration of 40 μM HZC, accompanied by the highest apoptosis rate. When cells were incubated with HZC at concentrations lower than 40 μM, the effect of apoptosis induction was increased with the increase of HZC concentration. When cells were incubated with HZC at concentrations higher than 40 μM, the effect of apoptosis induction of HepG2 cells decreased with the increase of HZC concentration (all $P < 0.05$; **Figure 3b,e**). Compared with the 20 μM CUR group, the apoptosis rate of HepG2

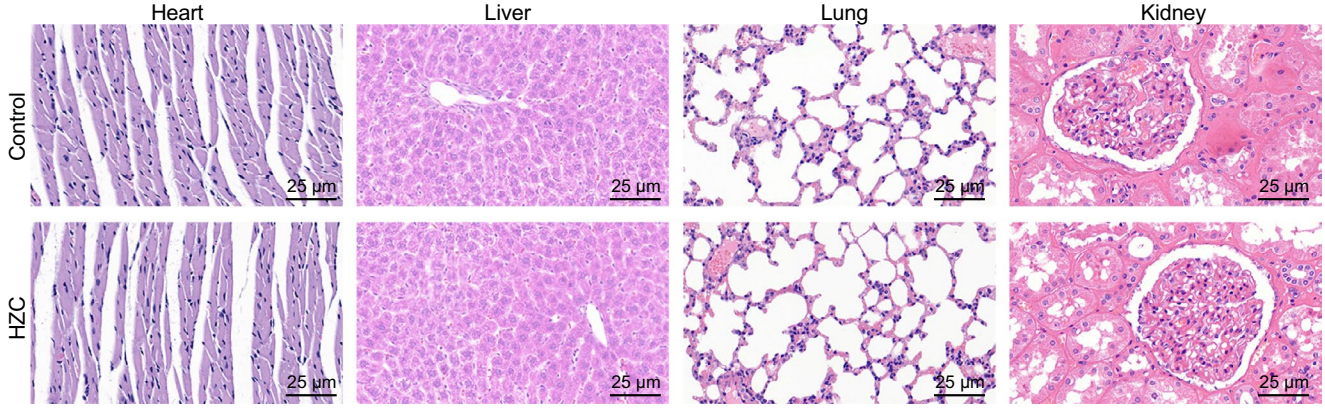

Figure 2 No histopathological changes in heart, liver, lung, and kidney tissues of mice in response to hydrazinocurcumin (HZC) treatment, according to hematoxylin-eosin staining (×400).

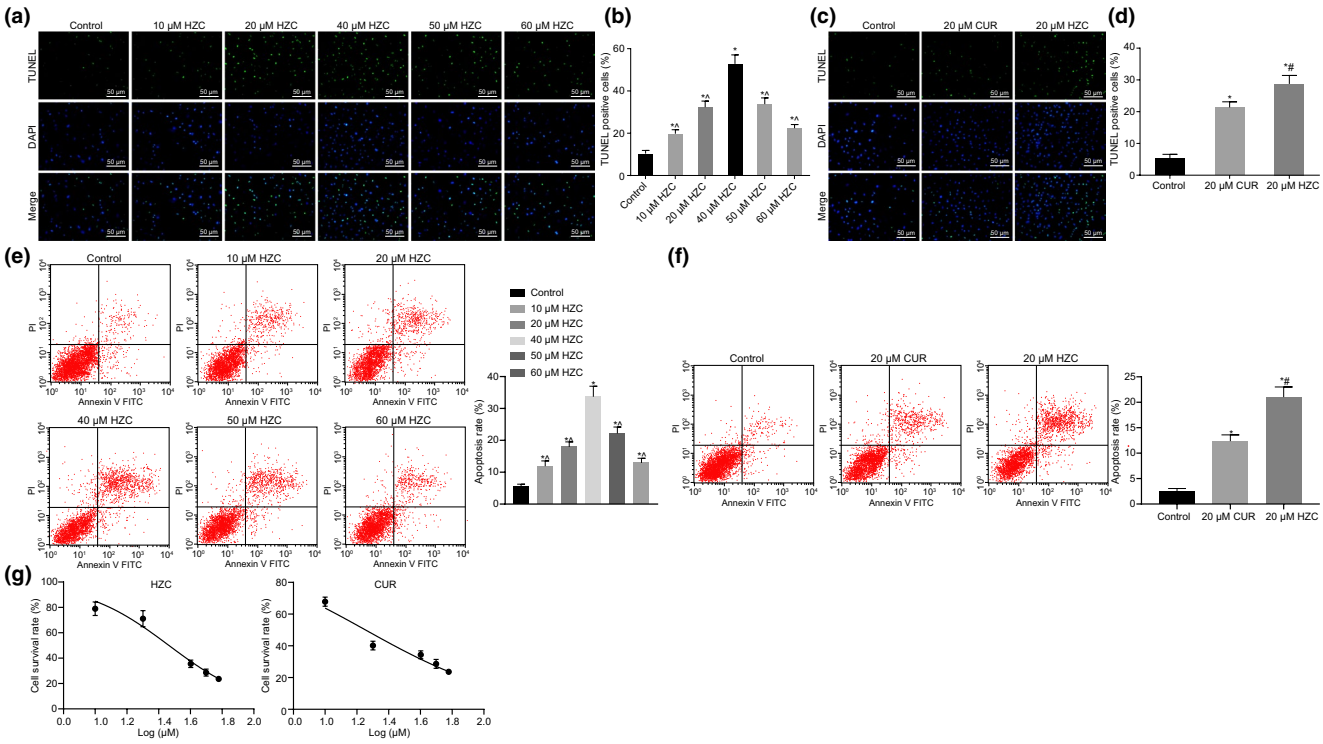

Figure 3 Hydrazinocurcumin (HZC) of 40 μM exerts the strongest promotive effect on apoptosis of HepG2 cells. (**a,b**) representative images and quantitative analysis of HepG2 cell apoptosis in response to treatment with different concentrations of HZC assessed by TUNEL staining (×200); (**c,d**) representative images and quantitative analysis of HepG2 cell apoptosis in response to 20 μM curcumin (CUR) and 20 μM HZC detected by TUNEL staining (×200); (**e**) HepG2 cell apoptosis upon treatment with different concentrations of HZC assessed by flow cytometry; (**f**) HepG2 cell apoptosis upon treatment with 20 μM CUR and 20 μM HZC assessed by flow cytometry; (**g**) half maximal inhibitory concentration values of cells treated with different concentrations of CUR and HZC measured by EdU assay. The experiment was repeated three times to obtain the mean value. The above results were measurement data and expressed as mean ± SD. The comparisons among multiple groups were tested by one-way analysis of variance; $^{*}P < 0.05$ vs. the control group; $^{\#}P < 0.05$ vs. the 20 μM CUR group; $^{\wedge}P < 0.05$ vs. the 40 μM HZC group. FITC, fluorescein isothiocyanate.

cells in the 20 μM HZC group was much higher, with significantly elevated apoptotic cells ($P < 0.05$; **Figure 3d,f**). In addition, the half maximal inhibitory concentration values of CUR and HZC were calculated to be 17.96 μM and 29.16 μM, respectively (**Figure 3g**). Therefore, the 40 μM dosage of HZC was chosen to treat HepG2 cells.

HZC inhibits proliferation, promotes apoptosis, and damages the structure of HepG2 cells through the p38 MAPK pathway

Ultrastructural electron microscopy (**Figure 4a**) was used to analyze the effects of HZC, 5-FU, and p38 MAPK pathway on the apoptosis, proliferation, and cell cycles of HepG2 cells. It was observed that cell morphology was irregular and the nucleus was larger with an increased nucleus to plasma ratio in the control group. There were no degenerated organelles in the cells, and the density of cytoplasm matrix was homogeneous. In the HZC and 5-FU groups, the nuclei were smaller with reduced, condensed, or even disappeared nucleolus, whereas the heterochromatin in the nucleus was increased, and the nuclei were aggregated along the edge of the nuclear membrane. In addition, the cytoplasm was filled with vacuoles of different sizes, and was partially dissolved with the appearance of autophagic bodies. Meanwhile, the SB203580 group exhibited normal nuclear morphology, no degenerated organelles in the cells, and homogeneous cytoplasm matrix density. The HZC + SB203580 group displayed regular nuclear morphology in most cells, and degenerated and atrophic organelles in a few cells.

Moreover, EdU assay (**Figure 4b,c**) and TUNEL assay (**Figure 4d,e**) demonstrated that HepG2 cells exhibited decreased proliferation and increased apoptosis of HepG2 cells in the HZC and 5-FU groups ($P < 0.05$), whereas HZC exerted stronger effects compared with 5-FU ($P < 0.05$). Additionally, relative to the control group, the SB203580 group exhibited reduced HepG2 cell apoptosis and increased HepG2 cell proliferation, whereas the HZC + SB203580 group showed similar trends ($P < 0.05$), indicating that the individual effects of HZC were reversed by a combination of HZC and SB203580.

Furthermore, the findings of RT-qPCR and Western blot assays displayed that the mRNA and protein expressions of p53 and caspase 3 were upregulated in HepG2 cells in the HZC and 5-FU groups, along with reduced pro-caspase 3 protein level ($P < 0.05$). Relative to the HZC group, the mRNA and protein expressions of p53 and caspase 3 were lower in the 5-FU group, accompanied by higher pro-caspase 3 protein level ($P < 0.05$), whereas the SB203580 group also exhibited decreased mRNA and protein expressions of p53

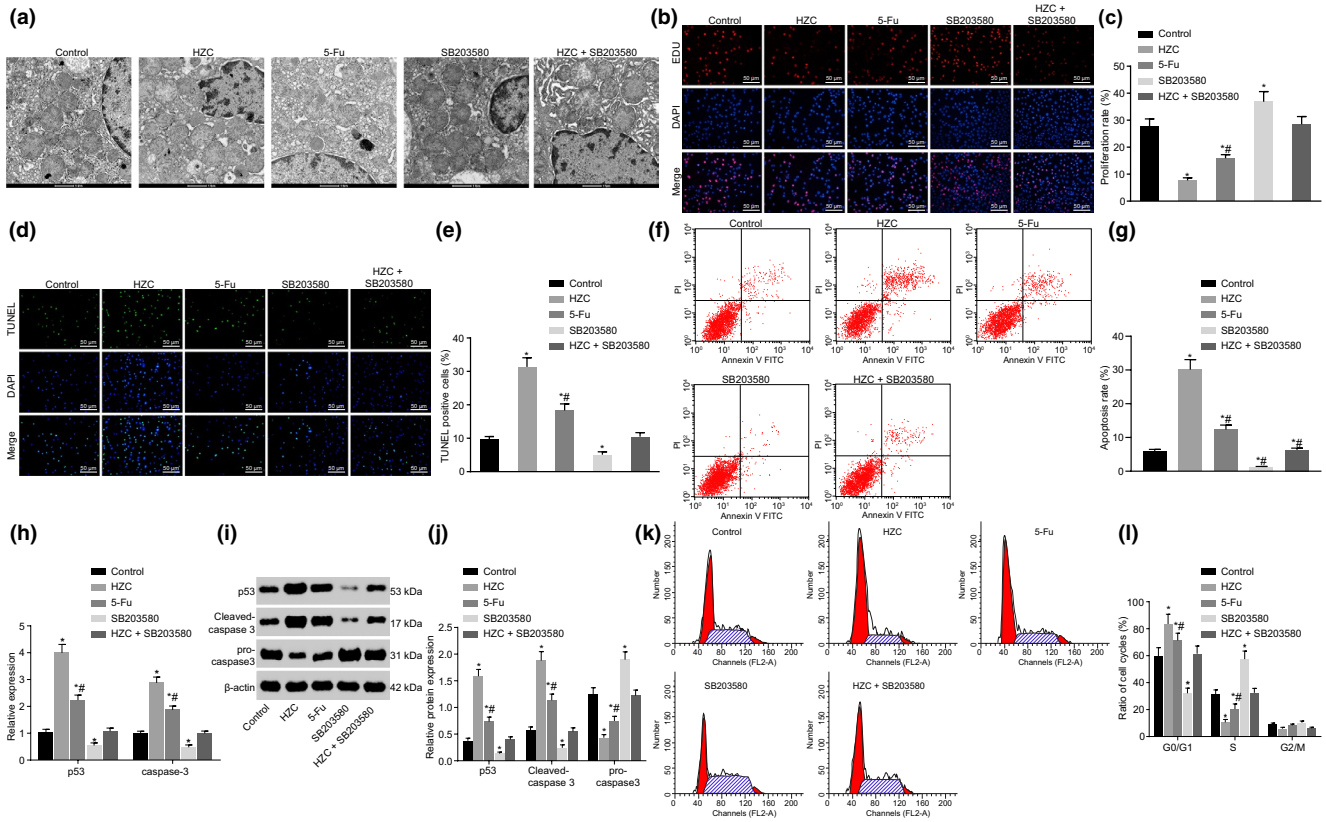

Figure 4 Hydrazinocurcumin (HZC) promotes apoptosis, inhibits proliferation, and damages the structure of HepG2 cells through the p38 MAPK pathway. (**a**) Ultrastructure of HepG2 cells in each group observed by ultrastructural electron microscopy; (**b,c**) representative images and statistical results of proliferation of HepG2 cells in each group examined by EdU assay (×200); (**d,e**) representative images and statistical results of apoptosis of HepG2 cells in each group determined by TUNEL staining (×200); (**f,g**) apoptosis of HepG2 cells in each group determined by flow cytometry; (**h**) the mRNA expression of p53 and cleaved caspase 3 of HepG2 cells in each group examined by reverse transcription quantitative polymerase chain reaction; (**i,j**) protein bands and quantitative analysis for the protein expression of p53, pro-caspase 3, and cleaved caspase 3 in HepG2 cells examined by Western blot assay; (**k,l**) cell cycle distribution of HepG2 cells examined by flow cytometry. The above results were measurement data and expressed as mean ± SD. The comparisons among multiple groups were examined by one-way analysis of variance (ANOVA), and the cell cycle of different groups was analyzed by repeated measures ANOVA; $^{*}P < 0.05$ vs. the control group; $^{\#}P < 0.05$ vs. the HZC group. 5-FU, 5-fluorouracil; FITC, fluorescein isothiocyanate.

and caspase 3, accompanied by diminished pro-caspase 3 protein level ($P < 0.05$; **Figure 4h–j**), and the individual effect of HZC was reversed by the combined effect of HZC and SB203580.

Additionally, the flow cytometric data of apoptosis (**Figure 4f,g**) and cell cycle distribution (**Figure 4k,l**) demonstrated that the HZC group and 5-FU group exhibited increased cells arrested at the G_0/G_1 phase and reduced cells at the S phase compared with the control group, corresponding to enhanced apoptosis ($P < 0.05$). Relative to the HZC group, the 5-FU and SB203580 groups displayed fewer cells at the G_0/G_1 phase and increased cells at the S phase ($P < 0.05$), with similar results detected in the HZC + SB203580 group, corresponding to suppressed apoptosis ($P < 0.05$). No significant differences were detected in regard to the cells arrested at the G2/M phase (all $P > 0.05$). Therefore, it was inferred that HZC could induce apoptosis, decrease proliferation, and damage the structure of HepG2 cell, whose effects were much stronger than 5-FU.

HZC or 5-FU activates the p38 MAPK pathway in HepG2 cells

RT-qPCR (**Figure 5a**) showed that, in contrast to the control group, the mRNA expressions of p38, ERK, and JNK in HepG2 cells were significantly upregulated in the HZC and 5-FU groups (all $P < 0.05$), with the HZC group exhibiting stronger upregulation of these factors ($P < 0.05$). Meanwhile, the mRNA expressions of p38, ERK, and JNK in HepG2 cells were repressed in the SB203580 group, and the combined treatment of HZC and SB203580 weakened the effect of HZC on these factors ($P < 0.05$). In addition, Western blot analysis (**Figure 5b,c**) revealed that compared with the control group, p-p38/t-p38, p-ERK/t-ERK, and p-JNK/t-JNK in HepG2 cells were significantly increased in the HZC group and 5-FU groups (all $P < 0.05$), and these ratios were significantly higher in the HZC group (all $P < 0.05$). Whereas, the SB203580 group displayed inhibited p-p38/t-p38, p-ERK/t-ERK, and p-JNK/t-JNK in HepG2 cells, and the effects of HZC on these ratios were reversed by the combined treatment of HZC and SB203580 (all $P < 0.05$).

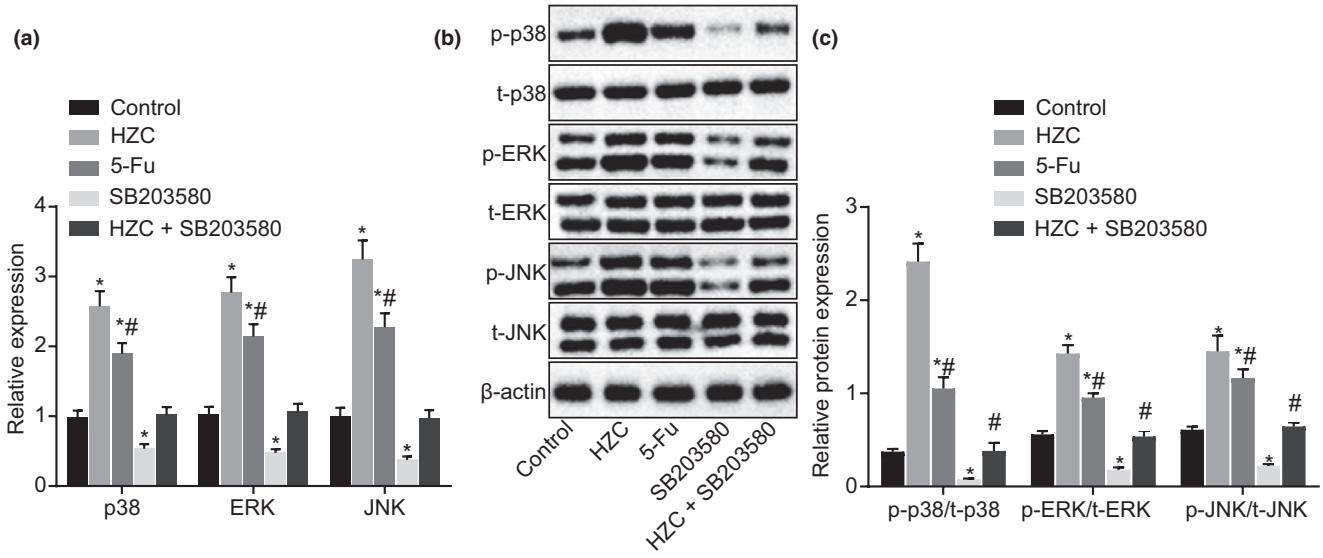

Figure 5 Hydrazinocurcumin (HZC) and 5-fluorouracil (5-FU) activates the p38 MAPK pathway in HepG2 cells. (**a**) The mRNA expression of p38, extracellular signal-regulated kinase (ERK) and Jun N-terminal kinase (JNK) in HepG2 cells examined by reverse transcription quantitative polymerase chain reaction; (**b**) the gray value of p38, p-ERK, t-ERK, p-JNK, and t-JNK protein bands in HepG2 cells examined by Western blot analysis; (**c**) statistical results of Western blot analysis. The above results were measurement data and expressed as mean ± SD. The comparisons among multiple groups were examined by one-way analysis of variance. $^{*}P < 0.05$ vs. the control group; $^{\#}P < 0.05$ vs. the HZC group.

Thus, it was suggested that both HZC and 5-FU induced the activation of p38 MAPK pathway to affect HepG2 cells.

HZC inhibits tumor growth in nude mice through the p38 MAPK pathway

The current study also evaluated the effects of HZC on tumor growth in nude mice with HCC. Tumor growth curves in nude mice (**Figure 6a**) displayed that both the HZC and 5-FU groups exerted inhibitory effects on tumor growth ($P < 0.05$), with HZC producing a much stronger inhibitory effect ($P < 0.05$), whereas the SB203580 group exerted a promoting effect on tumor growth ($P < 0.05$). The tumor weight of nude mice is shown in **Figure 6b,c**, and was determined to be reduced in the HZC and 5-FU groups while showing an increase in the SB203580 group compared with the control group ($P < 0.05$), whereas the effect of HZC on tumor weight was reversed in the HZC + SB203580 group. Compared with the HZC group, the tumor weight was significantly higher in the 5-FU group ($P < 0.05$). In addition, the results of TUNEL staining (**Figure 6d,e**) demonstrated that apoptotic cells were stained by brown coloration with clustered or fragmented nucleus and condensed chromatin. Apoptotic cells were irregular or few in the control group, whereas a large number of apoptotic cells were observed in the HZC and 5-FU groups (all $P < 0.05$). Apoptosis levels were significantly increased in the HZC and 5-FU groups, with highest values in the HZC group (all $P < 0.05$). Meanwhile, the SB203580 group exhibited decreased apoptosis levels, and the impact of HZC on apoptosis was reversed in the HZC + SB203580 group (all $P < 0.05$). Moreover, PCNA-positive cell levels were regarded as an indicator of the proliferation. Immunohistochemistry (**Figure 6f,g**) revealed that the positive rate of PCNA was significantly lower in the HZC and 5-FU groups compared with the control group ($P < 0.05$), and the positive rate of PCNA protein was much lower in the HZC group than that in the 5-FU group ($P < 0.05$). Expectedly, the SB203580 group displayed increased positive rate of PCNA protein, and the impact of HZC on the positive rate of PCNA protein was overturned in the HZC + SB203580 group ($P < 0.05$). Western blot analysis demonstrated an increase in the protein expression of cleaved PARP and cleaved caspase 3 along with the extent of p38 and JUN phosphorylation in the HZC group and the 5-FU group in comparison with the control group ($P < 0.05$). Meanwhile, the 5-FU group showed diminished protein expression of cleaved PARP and cleaved caspase 3 along with the extent of p38 and JUN phosphorylation, as compared with the HZC group ($P < 0.05$). Whereas, the SB203580 group exhibited reduced protein expression of cleaved PARP and cleaved caspase 3 along with extent of p38 and JUN phosphorylation, whereas all these effects were abolished in the HZC + SB203580 group ($P < 0.05$; **Figure 6h,i**). Detection results of the biochemical indexes of liver and kidneys of nude mice in each group showed that the drugs in each group exerted no obvious toxic effects on the nude mice (**Table 1**). These results revealed that HZC decreased proliferation and increased apoptosis of HCC tissues, and inhibited the growth of tumor in nude mice more effectively than 5-FU through the p38 MAPK pathway.

DISCUSSION

HCC cells proliferate, invade, and metastasize through a variety of signaling pathways during tumor progression.[19] In the current study, we uncovered that HZC could promote the activation of the p38 MAPK pathway, then potentiating apoptosis of HepG2 cells and ultimately retarding the progression of HCC.

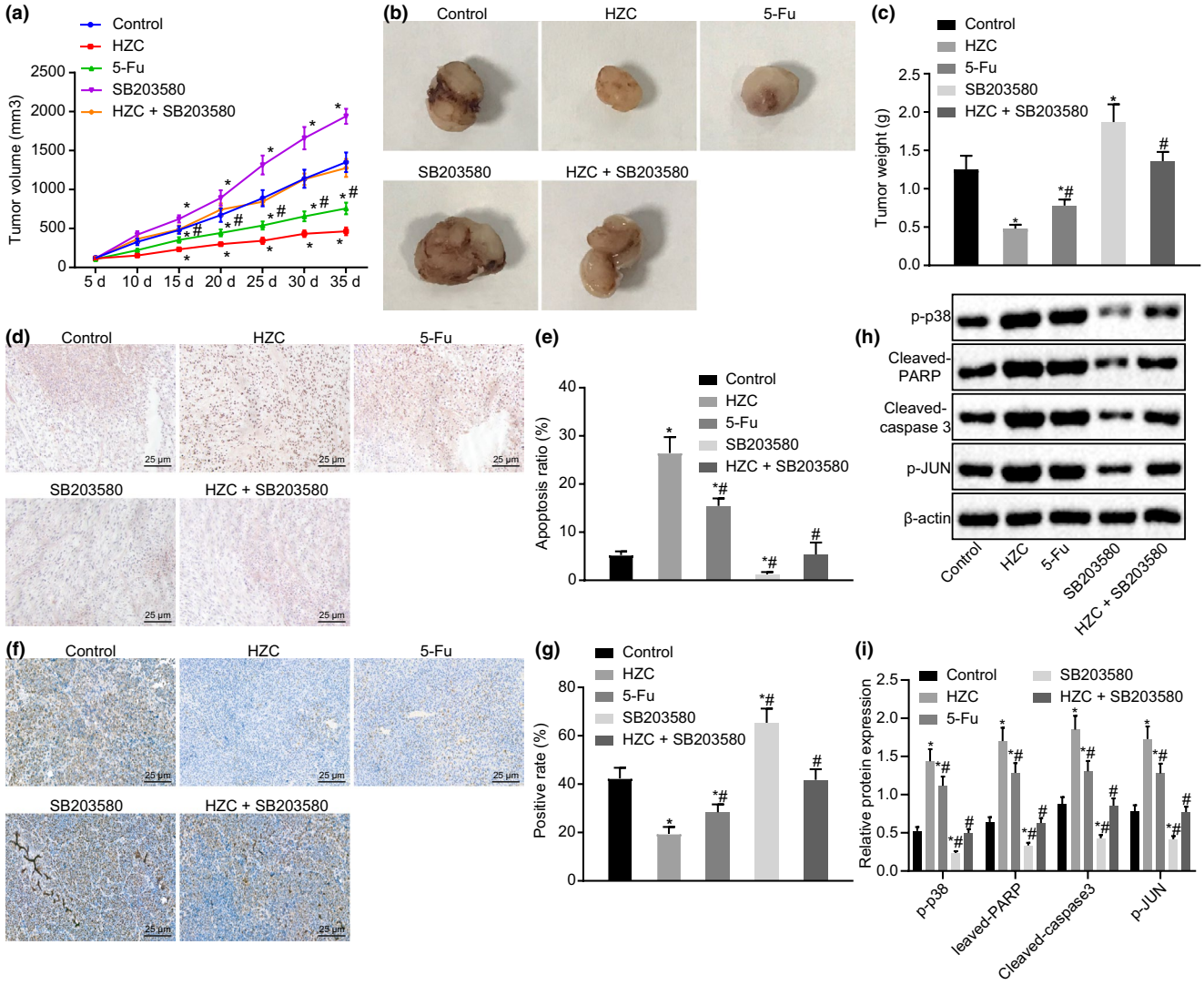

Figure 6 Hydrazinocurcumin (HZC) suppresses proliferation and promotes apoptosis of tumor growth in nude mice through the p38 MAPK pathway. (**a**) The growth curve of tumors in nude mice in each group (n = 5); (**b**) tumor weight of nude mice in each group; (**c**) statistical analysis of the tumor weight of nude mice in each group (n = 5); (**d**) TUNEL staining reflecting apoptosis level of tumor tissue of nude mice in each group (n = 5; ×400); (**e**) statistical analysis of TUNEL staining; (**f**) positive rate of proliferating cell nuclear antigen in tumor tissue of nude mice examined by immunohistochemistry (n = 5; ×400); (**g**) statistical analysis of immunohistochemistry; (**h,i**) Western blot analysis of cleaved PARP and cleaved caspase 3 proteins as well as the extent of p38 and JUN phosphorylation in each group. The above results were measurement data and expressed as mean ± SD. The results among multiple groups were examined by one-way analysis of variance (ANOVA). Repeated measures ANOVA was used to compare the results at different time points; $^{*}P < 0.05$ vs. the control group; $^{\#}P < 0.05$ vs. the HZC group. 5-FU, 5-fluorouracil.

Table 1 Quantitative analysis for biochemical indexes of nude mice in each group

Index	Control group	HZC group	5-Fu group	SB203580 group	HZC + SB203580 group
ALT, U/L	23.61 ± 2.26	26.01 ± 2.54	25.45 ± 2.23	28.37 ± 2.84	27.19 ± 2.8
AST, U/L	63.1 ± 6.39	65.53 ± 7.29	64.69 ± 7.58	70.33 ± 6.26	68.47 ± 5.97
CRE, umol/L	55.35 ± 3.94	59.29 ± 6.06	51.28 ± 5.29	60.27 ± 6.93	58.7 ± 5.99
ALB, g/L	32.9 ± 3.16	32.84 ± 3.29	36.56 ± 4.01	39.55 ± 4.75	39.91 ± 3.83
BUN, mmol/L	7.7 ± 1.21	7.54 ± 0.97	7.61 ± 0.89	7.49 ± 1.03	7.78 ± 0.92
TBL, mg/dL	1.61 ± 0.21	1.69 ± 0.17	1.8 ± 0.19	1.74 ± 0.18	1.91 ± 0.30

ALB, albumin; ALT, alanine aminotransferase; AST, aspartate aminotransferase; BUN, blood urea nitrogen; CRE, creatinine; HZC, hydrazinocurcumin; TBL, total bilirubin.

CUR, a polyphenol compound isolated from turmeric rhizome is well-known to possess abilities to inhibit the proliferation of various tumor cells.[20] Currently, low bioavailability hinders the widespread application of CUR in chemotherapy, but the advent of techniques allowing the synthesis of CUR analogues might solve that problem.[21] HZC, a novel CUR derivative, has been previously demonstrated to have the potential to inhibit the proliferation of bovine aortic endothelial cells at nanomolar concentrations (IC50 = 520 nM) without causing cytotoxicity,[22] which was in partial agreement with our findings; HZC post-isolation exerted little to no toxicity *in vivo*. In addition, our results indicated that HZC exerts a much stronger effect on the elicitation of HepG2 cell apoptosis compared with CUR. Similarly, a former investigation documented that HZC reduced the migration and invasive abilities of MDA-MB-231 and MCF-7 cells much more effectively than CUR.[21] Additionally, our findings revealed that HZC exerts a superior inhibitory effect on cell biological functions than 5-FU, which also demonstrates anticancer functions in HCC.[23]

Interestingly, evidence has also shown that CUR promotes apoptosis-associated mitochondrial membrane potential and intracellular free Ca^{2+} concentration in HepG2 cells.[24] In addition, another study demonstrated that CUR perturbs cell cycle distribution in HepG2 cells through means of cytoskeletal alignment.[25] Moreover, our findings indicated that HZC could inhibit proliferation, induce apoptosis, and damage the cell structure of HepG2 cells much more effectively than CUR. We also discovered that the inhibitory function of HZC was exerted in a dose-dependent manner. Similarly, Arif *et al.* illustrated that HZC treatment attenuated tumor growth in nude mice with oral cancer, partly resulting from the induction of cell apoptosis, which is in accordance with our findings.[26] Furthermore, we found that HZC and 5-FU upregulated the expressions of p53 and caspase 3 and downregulated that of pro-caspase 3, all of which have been previously demonstrated to regulate tumor development.[27,28]

More importantly, the current study uncovered the involvement of the p38 MAPK pathway in the functioning and underlying mechanisms of HZC on HCC cells. Members of the p38 MAPK family operate in a context-specific and type-specific manner to integrate signals that affect proliferation, differentiation, survival, and migration.[29] In addition, Kim *et al.* also reported that sauchinone elicits apoptosis of Hun-7 cells by activating the JNK/p38 pathway.[30] A recent study further demonstrated the capacity of S100A9 to trigger the growth and invasion of HCC through receptor for advanced glycation end products mediated ERK1/2 and p38 MAPK pathway.[31] Furthermore, it was found that honokiol activated p38 MAPK pathway and caspase-3 to induce apoptosis in HCC.[32] These studies were consistent with our study supporting that activation of the p38 MAPK pathway could induce apoptosis in HCC.

In summary, our findings demonstrated that HZC could induce apoptosis of HCC cells through a molecular mechanism associated with the p38 MAPK pathway. Nevertheless, further studies based on human specimens are warranted to confirm the underlying molecular mechanism and to minimize possible adverse events of HZC in clinical treatment of HCC.

Supporting Information. Supplementary information accompanies this paper on the *Clinical and Translational Science* website (www.cts-journal.com).

Supplementary Tables. Tables S1–S3.

Funding. This work was supported by Natural Science Foundation of Hebei Province (H2015206270) and Hebei Provincial Government Funded Special Funds for Clinical Medical Talents in 2017.

Conflict of Interest. The authors declared no competing interests for this work.

Author Contributions. Z.L.Z., Y.M.J., and C.Z. wrote the manuscript. H.T.H., K.Y.Q., C.W., and W.H.Y. designed the research. H.T.H. and Z.X. performed the research. L.P. analyzed the data. K.Y.Q. and L.P. contributed new reagents/analytical tools.

1. Palliyaguru, D.L. & Wu, F. Global geographical overlap of aflatoxin and hepatitis C: controlling risk factors for liver cancer worldwide. *Food Addit. Contam. Part A Chem. Anal. Control. Expo. Risk Assess.* **30**, 534–540 (2013).
2. Alshati, A., Bellapravalu, S., Srinivasan, I., Nadir, A. & Chuang, K.Y. Imaging-negative hepatocellular carcinoma presents as an intrabiliary mass. *ACG Case Rep. J.* **6**, e00068 (2019).
3. Maluccio, M. & Covey, A. Recent progress in understanding, diagnosing, and treating hepatocellular carcinoma. *CA Cancer J. Clin.* **62**, 394–399 (2012).
4. Huang, G. *et al.* Isoquercitrin inhibits the progression of liver cancer in vivo and in vitro via the MAPK signalling pathway. *Oncol. Rep.* **31**, 2377–2384 (2014).
5. Lin, L. *et al.* Depletion of Cks1 and Cks2 expression compromises cell proliferation and enhance chemotherapy-induced apoptosis in HepG2 cells. *Oncol. Rep.* **35**, 26–32 (2016).
6. Zeng, J. *et al.* Sasanquasaponin from Camellia oleifera Abel. induces apoptosis via Bcl-2, Bax and caspase-3 activation in HepG2 cells. *Mol. Med. Rep.* **12**, 1997–2002 (2015).
7. Shi, J.J. *et al.* Guggulsterone induces apoptosis of human hepatocellular carcinoma cells through intrinsic mitochondrial pathway. *World J. Gastroenterol.* **21**, 13277–13287 (2015).
8. Zhao, X., Jiang, K., Liang, B. & Huang, X. Anticancer effect of xanthohumol induces growth inhibition and apoptosis of human liver cancer through NF-kappaB/p53-apoptosis signaling pathway. *Oncol. Rep.* **35**, 669–675 (2016).
9. Shu, G. *et al.* Isoliensinine, a bioactive alkaloid derived from embryos of *Nelumbo nucifera*, induces hepatocellular carcinoma cell apoptosis through suppression of NF-kappaB signaling. *J. Agric. Food Chem.* **63**, 8793–8803 (2015).
10. Tan, Y., Leonhard, M., Moser, D., Ma, S. & Schneider-Stickler, B. Antibiofilm efficacy of curcumin in combination with 2-aminobenzimidazole against single- and mixed-species biofilms of Candida albicans and Staphylococcus aureus. *Colloids Surf. B Biointerfaces* **174**, 28–34 (2019).
11. Zhou, H., Beevers, C.S. & Huang, S. The targets of curcumin. *Curr. Drug Targets* **12**, 332–347 (2011).
12. Rathore, R., Jain, J.P., Srivastava, A., Jachak, S.M. & Kumar, N. Simultaneous determination of hydrazinocurcumin and phenol red in samples from rat intestinal permeability studies: HPLC method development and validation. *J. Pharm. Biomed. Anal.* **46**, 374–380 (2008).
13. Zhang, X. *et al.* Hydrazinocurcumin encapsuled nanoparticles "re-educate" tumor-associated macrophages and exhibit anti-tumor effects on breast cancer following STAT3 suppression. *PLoS One* **8**, e65896 (2013).
14. Kapakos, G., Youreva, V. & Srivastava, A.K. Cardiovascular protection by curcumin: molecular aspects. *Indian J. Biochem. Biophys.* **49**, 306–315 (2012).
15. Sun, B., Zhang, X., Yonz, C. & Cummings, B.S. Inhibition of calcium-independent phospholipase A2 activates p38 MAPK signaling pathways during cytostasis in prostate cancer cells. *Biochem. Pharmacol.* **79**, 1727–1735 (2010).
16. Jiao, J.W. & Wen, F. Tanshinone IIA acts via p38 MAPK to induce apoptosis and the down-regulation of ERCC1 and lung-resistance protein in cisplatin-resistant ovarian cancer cells. *Oncol. Rep.* **25**, 781–788 (2011).
17. Zhao, J.A. *et al.* Preventive effect of hydrazinocurcumin on carcinogenesis of diethylnitrosamine-induced hepatocarcinoma in male SD rats. *Asian Pac. J. Cancer Prev.* **15**, 2115–2121 (2014).
18. Zhang, Z.J., Yang, Y.K. & Wu, W.Z. Bufalin attenuates the stage and metastatic potential of hepatocellular carcinoma in nude mice. *J. Transl. Med.* **12**, 57 (2014).
19. Tian, T. *et al.* PTEN inhibits the migration and invasion of HepG2 cells by coordinately decreasing MMP expression via the PI3K/Akt pathway. *Oncol. Rep.* **23**, 1593–1600 (2010).

20. Ferguson, J.E. & Orlando, R.A. Curcumin reduces cytotoxicity of 5-Fluorouracil treatment in human breast cancer cells. *J. Med. Food* **18**, 497–502 (2015).
21. Wang, X., Zhang, Y., Zhang, X., Tian, W., Feng, W. & Chen, T. The curcumin analogue hydrazinocurcumin exhibits potent suppressive activity on carcinogenicity of breast cancer cells via STAT3 inhibition. *Int. J. Oncol.* **40**, 1189–1195 (2012).
22. Shim, J.S. *et al.* Hydrazinocurcumin, a novel synthetic curcumin derivative, is a potent inhibitor of endothelial cell proliferation. *Bioorg. Med. Chem.* **10**, 2987–2992 (2002).
23. Zhao, L. *et al.* Synergistic effect of 5-fluorouracil and the flavanoid oroxylin A on HepG2 human hepatocellular carcinoma and on H22 transplanted mice. *Cancer Chemother. Pharmacol.* **65**, 481–489 (2010).
24. Wang, M., Ruan, Y., Chen, Q., Li, S., Wang, Q. & Cai, J. Curcumin induced HepG2 cell apoptosis-associated mitochondrial membrane potential and intracellular free Ca(2+) concentration. *Eur. J. Pharmacol.* **650**, 41–47 (2011).
25. Jiang, J., Jin, H., Liu, L., Pi, J., Yang, F. & Cai, J. Curcumin disturbed cell-cycle distribution of HepG2 cells via cytoskeletal arrangement. *Scanning* **35**, 253–260 (2013).
26. Arif, M. *et al.* Nitric oxide-mediated histone hyperacetylation in oral cancer: target for a water-soluble HAT inhibitor, CTK7A. *Chem. Biol.* **17**, 903–913 (2010).
27. Giorgi, C. *et al.* p53 at the endoplasmic reticulum regulates apoptosis in a Ca2+-dependent manner. *Proc. Natl. Acad. Sci. USA* **112**, 1779–1784 (2015).
28. Hu, Q. *et al.* Elevated cleaved caspase-3 is associated with shortened overall survival in several cancer types. *Int. J. Clin. Exp. Pathol.* **7**, 5057–5070 (2014).
29. Wagner, E.F. & Nebreda, A.R. Signal integration by JNK and p38 MAPK pathways in cancer development. *Nat. Rev. Cancer* **9**, 537–549 (2009).
30. Kim, Y.W., Jang, E.J., Kim, C.H. & Lee, J.H. Sauchinone exerts anticancer effects by targeting AMPK signaling in hepatocellular carcinoma cells. *Chem. Biol. Interact.* **261**, 108–117 (2017).
31. Wu, R. *et al.* S100A9 promotes human hepatocellular carcinoma cell growth and invasion through RAGE-mediated ERK1/2 and p38 MAPK pathways. *Exp. Cell Res.* **334**, 228–238 (2015).
32. Deng, J. *et al.* Involvement of p38 mitogen-activated protein kinase pathway in honokiol-induced apoptosis in a human hepatoma cell line (hepG2). *Liver Int.* **28**, 1458–1464 (2008).